

PAPER • OPEN ACCESS

Band tailoring by annealing and current conduction of Co-doped ZnO transparent resistive switching memory

To cite this article: Debashis Panda *et al* 2021 *IOP Conf. Ser.: Mater. Sci. Eng.* **1034** 012140

View the [article online](#) for updates and enhancements.



240th ECS Meeting ORLANDO, FL

Orange County Convention Center Oct 10-14, 2021



Abstract submission due: April 9

SUBMIT NOW

Band tailoring by annealing and current conduction of Co-doped ZnO transparent resistive switching memory

Debashis Panda¹, Firman Mangasa Simanjuntak², Alaka Pradhan¹, Femiana Gapsari³, Themis Prodromakis^{2**}

1 Dept. of Physics, National Institute of Science and Technology

Berhampur, Orissa, India

*Email: phy.dpanda@gmail.com

2 Centre for Electronics Frontiers, University of Southampton, SO171BJ, UK

**Email: t.prodromakis@soton.ac.uk

3 Dept. of Mechanical Engineering, Brawijaya University

Malang 65145, Indonesia

IOP Conf. Ser.: Mater. Sci. Eng. **1034** 012140

IOP Conf. Ser.: Mater. Sci. Eng. 1034 012140

Abstract. The switching characteristics of ITO/Zn_{1-x}Co_xO/ITO transparent resistive random access memories were studied. 5 mol% cobalt doped ZnO resistive layer improves bipolar switching properties. In addition, the redshift in band energy caused by doping of cobalt (Co) was studied. The doped memory device also showed a change in band energy by 0.1 eV when subjected to annealing of 400 °C. Annealing below 400 °C temperature did not show any characteristic changes. The film morphology analysis suggested the increase in roughness with annealing temperature, which can be seen from FESEM and AFM images. In this study annealing and Co doping effect on ZnO based non-volatile memory device is presented. Moreover, transparent memory devices with 90% transmittance at 550 nm wavelength have been reported. At low field and high field region Schottky emission and ionic conduction are dominated respectively.

Keywords: resistive switching memory, transparent device, doped ZnO, annealing effect, current conduction

1. Introduction

Transparent resistive switching memory (RRAM) has earned a tremendous attraction in transparent electronics as well as use in future non-volatile memory devices [1–6]. The selection of insulating active material in transparent Metal-Insulator-Metal (MIM)RRAM is very crucial as it is the main factor defining the device characteristics [7–14]. Due to the wide direct band gap of 3.3 eV, ZnO can be a potential active material for the transparent electronic devices as transparent RRAM [15,16]. The presence of excess native defects such as oxygen vacancies and zinc interstitials degrades the overall memory performance of pure ZnO [17–24]. The study suggests that the switching performance of RRAM can be improved by controlling the number of defects present, which governs the creation and annihilation of conductive filaments (CFs) in the RRAM [25–30].



Doping is often used to control the defect concentration. Co-doped ZnO(Co:ZnO) has gained a great interest in past years owing to its capability in the field of magnetic semiconductor applications [30–32]. To magnify the potential of Co-doped ZnO resistive switching for application in non-volatile memories (NVM), more studies should be performed on the electrical and other characteristics properties of these devices. Here, we report the annealing effect on the structural, optical, and switching properties of Co:ZnORRAM devices.

2. Methods

All films were deposited by RF sputtering for its low temperature and low cost fabrications as compared to other methods [2,33,34]. A CoO doped (5 mol. %) ZnO thin film of thickness 38-nm was sputtered at room temperature on a commercial indium tin oxide (ITO) coated glass substrate (Merck & Co., Inc.). During deposition the working pressure of 10 mTorr, rf power of 60W and Ar/O₂ gas flow ratio of 20/10 sccm, respectively were sternly maintained. A top electrode (TE) of ITO was sputtered at room temperature from ITO (purity 99.99 %) target at Ar ambient of 10 mTorr using a stainless-steel shadow mask having a diameter of 150 μm . Annealing of the sample was done at 200 °C, 300 °C, and 400 °C for 10 minutes to vary the native defects. The electrical switching properties and optical transparency of the devices were investigated by using a B1500A semiconductor device analyzer (Agilent Technologies, Inc.) and an UV-Vis spectrophotometer (UV-1800, Shimadzu), respectively. Atomic force microscopy (AFM) (VEECO Nanoscope IV) was investigated to observe the topography of the Co-doped ZnO film.

3. Result and discussion

Current-Voltage (I-V) switching curve of the said RRAM were measured by applying an external bias at the top electrode with grounded bottom electrode, shown in **Figure 1a**. By the application of positive voltage sweep, the device is turned into the low resistance state (LRS) from initial pristine high resistance state (HRS), which is named as forming process. In this given device, a forming voltage of 3.5 V is necessary to start the resistive switching. Bipolar resistive switching is observed in the device with the 1.2 V SET voltage of and the -1.7 V RESET voltage. A compliance current of 5 mA is maintained during measurement in order to evade the device breakdown. The switching curves are fitted with different conduction mechanisms in different regions (not shown here).

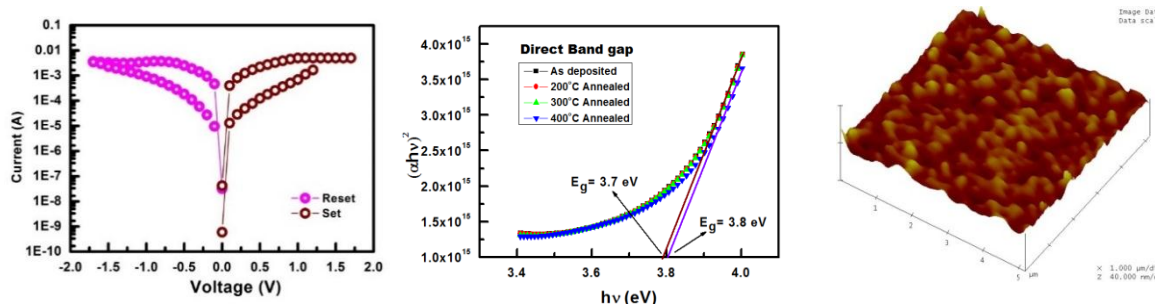


Figure 1. a) I-V switching curve; b) Tauc's plot of of ITO/Co:ZnO/ITO RRAM at different annealing; c) 3D AFM topography of 200° C annealed Co:ZnO surface.

The Tauc plot of the Co:ZnO sample at different annealing conditions obtained from the transmittance spectra as shown in **Figure 1b**. We can infer from the number that the device of ~ 390 nm thickness is very transparent in the visible region and suitable for the use in transparent

electronic devices. It is observed from the figure that the energy gap value of the device is 3.7 eV and 3.8 eV depending on the annealing temperature, which differs from the energy gap value of pristine ZnO (3.3 eV). This redshift of the energy band gap in the Co doped ZnO from the pristine one can be attributed to the effect of Co doping [35]. The strong sp-d exchange interaction between the band electrons and localized 'd' electrons are mainly responsible for the increase in the energy gap or band gap [36]. This results supported by the literature of oxide thin films grown by different techniques, where there is an increase of band gap in Co:ZnO is observed [35,36].

Singh *et al.* also explained the change in band gap in their Co-doped ZnO sample on the basis of the smaller ionic radius of Co ions compared to that of Zn [37]. A blue shift in absorption peak indicates an increase in band gap, which may be due to the enhances of carrier concentration by Burnstein–Moss effect [38]. The deviation in optical properties can be seen after the sample annealed at 400 °C. The annealing temperature of 200 °C and 300 °C had no or very minimal effect on the optical property and retained the same as the as-deposited sample.

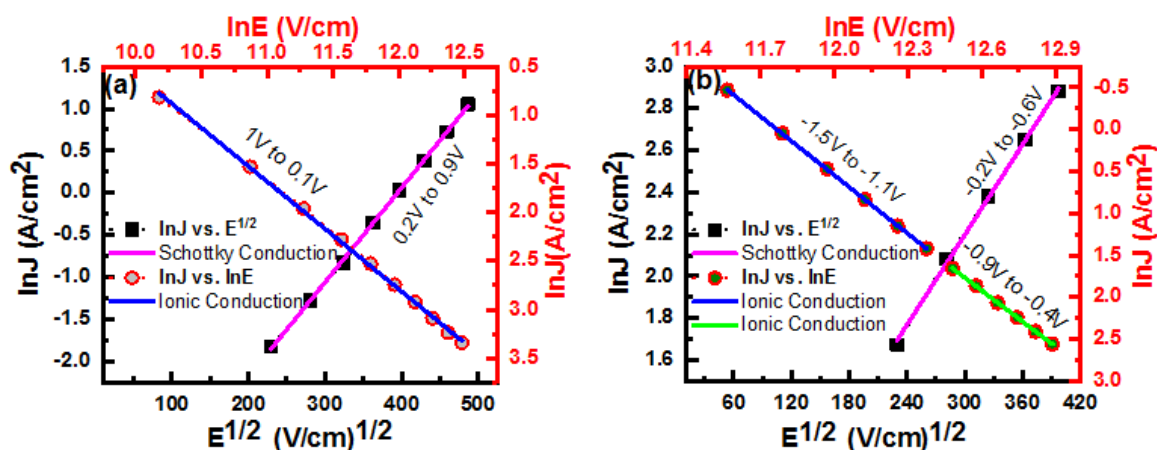


Figure 2. current conduction fittings of the a) LRS and b) HRS, indicating Schottky and ionic conduction mechanisms in low and high electric field region respectively.

From the figure we can infer that for the annealing temperature at 400 °C, a change in electrical energy band gap was found. The energy band gap of the device has increased to 3.8 eV from 3.7 eV when the samples are annealed at 400 °C. This increase in energy band gap may be accredited to the increase of the size of the particle with the increase of annealing temperature [39] and also can be due to the degradation of density of localized states during the annealing process [40]. The calculated band gap is also verified using the photo-luminescence study (not shown here). In order to know the size of the particle and surface morphology of the active layers, the AFM has been studied. **Figure 1c** shows the typical tapping mode AFM topography of Co:ZnO surface annealed at 200° C. The surface of the film is quite smooth (~2.3 nm); however, the roughness increases after annealing. The AFM topography corroborates with the FESEM surface morphology.

For exploring the current conduction mechanism of the ITO/Co:ZnO/ITO memory device, the set/ reset curves are fitted with all conduction mechanisms in different regions using the equations 1 and 2 [41], as shown in **Figure 2**.

$$\ln(J) = \left(\frac{q \sqrt{\frac{qE}{4\pi\epsilon_0\epsilon_r}}}{kT} \right) + \left(\ln A^* T^2 - \frac{q\phi_B}{kT} \right) \quad (1)$$

$$J = J_0 \exp\left[-\left(\frac{-q\phi_B}{kT} - \frac{Eqd}{2kT}\right)\right] \quad (2)$$

Where, J , q , ϵ_0 , ϵ_r , A^* , k , T , ϕ_B and d are the corresponding current density, the charge of an electron, permittivity in vacuum, relative dielectric constant, effective Richardson constant, Boltzmann's constant, temperature, the potential barrier height and jumping distance between two nearby defects respectively. All other symbols have their usual meaning.

It is undoubtedly found that the low electric field region is controlled by Schottky emission, which is mainly due to the jumping of electrons into the conduction band of the oxide after gaining sufficient energy [42]. However, at high electric field region, the conduction mechanism is governed by ionic conduction, which may be because of the shifting of oxygen vacancies by the application of the electric field inside the oxide material[43].

4. Conclusion

In conclusion, the optical properties of highly transparent ITO/Co:ZnO/ITO resistive memory devices were studied. Increase in the bandgap energy from 3.3 eV for pristine ZnO to 3.7 eV for Co:ZnO due to doping is reported. The response to 200 °C, 300 °C and 400 °C of the RRAM device resulted in a change in band energy. The energy increased to 3.8 eV from 3.7 eV when annealed in 400 °C and did not show any difference when annealed at lower temperatures of 200 °C and 300 °C with respect to pristine Co:ZnO device. The roughness of the surface increases with annealing temperature, which was analyzed by FESEM and AFM. Schottky emission is dominated in the low field region, whereas at high field ionic emission is dominated. This report not only showing an encouraging method of the upcoming transparent non-volatile memory using doping to improve the device property but also provides a brief understanding, which can be useful for the fabrication of next-generation non-volatile memories.

5. Acknowledgment

The authors thank Prof. Tseng Tseung-Yuen from the Institute of Electronics – National Chiao Tung University for the experimental support. D. Panda acknowledged the DST-SERB research grant, Govt. of India (Grant no: SRG/2019/000129) to support this work. F. M. Simanjuntak and T. Prodromakis acknowledge the support of EPSRC Programme Grant (EP/R024642/1) and H2020-FETPROACT-2018-01 SYNCH project.

6. References

- [1] Jung P-Y, Panda D, Chandrasekaran S, Rajasekaran S and Tseng T-Y 2020 Enhanced Switching Properties in TaO_x Memristors Using Diffusion Limiting Layer for Synaptic Learning *IEEE Journal of the Electron Devices Society* **8** 110–5
- [2] Simanjuntak F M, Panda D, Wei K and Tseng T 2016 Status and Prospects of ZnO-Based Resistive Switching Memory Devices *Nanoscale Research Letters* **11** 368
- [3] Panda D and Tseng T-Y 2013 One-dimensional ZnO nanostructures: fabrication, optoelectronic properties, and device applications *Journal of Materials Science* **48** 6849–77
- [4] Simanjuntak F M, Panda D, Tsai T-L, Lin C-A, Wei K-H and Tseng T-Y 2015 Enhanced switching uniformity in AZO/ZnO 1-x /ITO transparent resistive memory devices by bipolar double forming *Applied Physics Letters* **107** 033505

- [5] Chang L-Y, Simanjuntak F M, Hsu C-L, Chandrasekaran S and Tseng T-Y 2020 Suboxide interface induced digital-to-analog switching transformation in all Ti-based memristor devices *Applied Physics Letters* **117** 073504
- [6] Rajasekaran S, Simanjuntak F M, Panda D, Chandrasekaran S, Aluguri R, Saleem A and Tseng T-Y 2020 Fast, Highly Flexible, and Transparent TaO_x-Based Environmentally Robust Memristors for Wearable and Aerospace Applications *ACS Applied Electronic Materials* **acsaelm.0c00441**
- [7] Kumar S S, Sahu P P and Panda D 2017 Barrier Potential Engineering in Ti/HfO₂/Pt Resistive Random Access Memory *Journal of Nanoscience and Nanotechnology* **17** 9328–32
- [8] Simanjuntak F M, Ohno T, Chandrasekaran S, Tseng T-Y and Samukawa S 2020 Neutral oxygen irradiation enhanced forming-less ZnO-based transparent analog memristor devices for neuromorphic computing applications *Nanotechnology* **31** 26LT01
- [9] Simanjuntak F M, Chandrasekaran S, Lin C and Tseng T-Y 2019 ZnO₂/ZnO bilayer switching film for making fully transparent analog memristor devices *APL Materials* **7** 051108
- [10] Simanjuntak F M, Ohno T and Samukawa S 2019 Neutral Oxygen Beam Treated ZnO-Based Resistive Switching Memory Device *ACS Applied Electronic Materials* **1** 18–24
- [11] Simanjuntak F M, Ohno T and Samukawa S 2019 Influence of rf sputter power on ZnO film characteristics for transparent memristor devices *AIP Advances* **9** 105216
- [12] Simanjuntak F M, Chandrasekaran S, Gapsari F and Tseng T Y 2019 Switching and synaptic characteristics of AZO/ZnO/ITO valence change memory device *IOP Conference Series: Materials Science and Engineering* **494** 012027
- [13] Simanjuntak F M, Ohno T and Samukawa S 2019 Film-Nanostructure-Controlled Inerasable-to-Erasable Switching Transition in ZnO-Based Transparent Memristor Devices: Sputtering-Pressure Dependency *ACS Applied Electronic Materials* **1** 2184–9
- [14] Panda D, Simanjuntak F M and Tseng T-Y 2016 Temperature induced complementary switching in titanium oxide resistive random access memory *AIP Advances* **6** 075314
- [15] Chandrasekaran S, Simanjuntak F M, Panda D and Tseng T-Y 2019 Enhanced Synaptic Linearity in ZnO-Based Invisible Memristive Synapse by Introducing Double Pulsing Scheme *IEEE Transactions on Electron Devices* **66** 4722–6
- [16] Simanjuntak F M, Panda D, Tsai T-L, Lin C-A, Wei K-H and Tseng T-Y 2015 Enhancing the memory window of AZO/ZnO/ITO transparent resistive switching devices by modulating the oxygen vacancy concentration of the top electrode *Journal of Materials Science* **50** 6961–9
- [17] Cheng H C, Chen S W and Wu J M 2011 Resistive switching behavior of (Zn_{1-x}Mg_x)O films prepared by sol-gel processes *Thin Solid Films*
- [18] Chandrasekaran S, Simanjuntak F, Saminathan R, Panda D and Tseng T-Y 2019 Improving linearity by introducing Al in HfO₂ as memristor synapse device *Nanotechnology* **6** 107–13
- [19] Chandrasekaran S, Simanjuntak F M, Aluguri R and Tseng T 2018 The impact of TiW barrier layer thickness dependent transition from electro-chemical metallization memory to valence change memory in ZrO₂-based resistive switching random access memory devices *Thin Solid Films* **660** 777–81
- [20] Simanjuntak F M, Chandrasekaran S, Lin C-C and Tseng T-Y 2018 Switching Failure Mechanism in Zinc Peroxide-Based Programmable Metallization Cell *Nanoscale Research Letters* **13** 327
- [21] Singh P, Simanjuntak F M, Kumar A and Tseng T 2018 Resistive switching behavior of Ga doped ZnO-nanorods film conductive bridge random access memory *Thin Solid Films* **660** 828–33
- [22] Chandrasekaran S, Simanjuntak F M and Tseng T 2018 Controlled resistive switching characteristics of ZrO₂-based electrochemical metallization memory devices by modifying the thickness of the metal barrier layer *Japanese Journal of Applied Physics* **57** 04FE10

- [23] Simanjuntak F M, Singh P, Chandrasekaran S, Lumbantoruan F J, Yang C-C, Huang C-J, Lin C-C and Tseng T-Y 2017 Role of nanorods insertion layer in ZnO-based electrochemical metallization memory cell *Semiconductor Science and Technology* **32** 124003
- [24] Panda D, Simanjuntak F M, Chandrasekaran S, Pattanayak B, Singh P and Tseng T Y 2020 Barrier Layer Induced Switching Stability in Ga:ZnO Nanorods Based Electrochemical Metallization Memory *IEEE Transactions on Nanotechnology* 1–1
- [25] Panda D, Huang C Y and Tseng T Y 2012 Resistive switching characteristics of nickel silicide layer embedded HfO₂ film *Applied Physics Letters* **100**
- [26] Simanjuntak F M, Chandrasekaran S, Pattanayak B, Lin C-C and Tseng T-Y 2017 Peroxide induced volatile and non-volatile switching behavior in ZnO-based electrochemical metallization memory cell *Nanotechnology* **28** 38LT02
- [27] Chandrasekaran S, Simanjuntak F M, Tsai T-L, Lin C-A and Tseng T-Y 2017 Effect of barrier layer on switching polarity of ZrO₂-based conducting-bridge random access memory *Applied Physics Letters* **111** 113108
- [28] Simanjuntak F M, Pattanayak B, Lin C-C and Tseng T-Y 2017 Resistive Switching Characteristics of Hydrogen Peroxide Surface Oxidized ZnO-Based Transparent Resistive Memory Devices *ECS Transactions* **77** 155–60
- [29] Aluguri R, Kumar D, Simanjuntak F M and Tseng T-Y 2017 One bipolar transistor selector - One resistive random access memory device for cross bar memory array *AIP Advances* **7** 095118
- [30] Simanjuntak F M, Prasad O K, Panda D, Lin C-A, Tsai T-L, Wei K-H and Tseng T-Y 2016 Impacts of Co doping on ZnO transparent switching memory device characteristics *Applied Physics Letters* **108** 183506
- [31] Naeem M, Hasanain S K, Kobayashi M, Ishida Y, Fujimori A, Buzby S and Shah S I 2006 Effect of reducing atmosphere on the magnetism of Zn_{1-x}Co_xO (0 ≤ x ≤ 0.10) nanoparticles *Nanotechnology*
- [32] Lee H-J, Jeong S-Y, Cho C R and Park C H 2002 Study of diluted magnetic semiconductor: Co-doped ZnO *Applied Physics Letters* **81** 4020
- [33] Lumbantoruan F, Zheng X-X, Huang J-H, Huang R-Y, Mangasa F, Chang E-Y, Tu Y-Y and Lee C-T 2018 Structural and electrical properties analysis of InAlGaN/GaN heterostructures grown at elevated temperatures by MOCVD *Journal of Crystal Growth* **501** 7–12
- [34] Amrillah T, Chen Y X, Duong M N, Abdussalam W, Simanjuntak F M, Chen C H, Chu Y H and Juang J Y 2020 Effects of pillar size modulation on the magneto-structural coupling in self-assembled BiFeO₃-CoFe₂O₄ heteroepitaxy *CrystEngComm* **22** 435–40
- [35] Dhruvashi and Shishodia P K 2016 Effect of cobalt doping on ZnO thin films deposited by sol-gel method *Thin Solid Films*
- [36] Hammad T M, Salem J K and Harrison R G 2012 Structure, optical properties and synthesis of Co-doped ZnO superstructures *Applied Nanoscience* 133–9
- [37] Benramache S, Benhaoua B and Bentrah H 2013 Preparation of transparent, conductive ZnO:Co and ZnO:In thin films by ultrasonic spray method *Journal of Nanostructure in Chemistry* **3** 54
- [38] Singh J, Chanda A, Gupta S, Shukla P and Chandra V 2016 Effect of cobalt doping on structural and optical properties of ZnO nanoparticles p 050091
- [39] Ungula J, Dejene B F and Swart H C 2017 Effect of annealing on the structural, morphological and optical properties of Ga-doped ZnO nanoparticles by reflux precipitation method *Results in Physics*
- [40] El-Zahed H, Dongol M and Radwan M 2002 Annealing and thickness effect on the optical absorption of Ge₂₀Te₈₀ and Cu₆Ge₁₄Te₈₀ films *EPJ Applied Physics*
- [41] Roy S, Niu G, Wang Q, Wang Y, Zhang Y, Wu H, Zhai S, Shi P, Song S, Song Z, Ye Z G, Wenger C,

- Schroeder T, Xie Y H, Meng X, Luo W and Ren W 2020 Toward a Reliable Synaptic Simulation Using Al-Doped HfO₂ RRAM *ACS Applied Materials and Interfaces*
- [42] Loy D J J, Dananjaya P A, Hong X L, Shum D P and Lew W S 2018 Conduction Mechanisms on High Retention Annealed MgO-based Resistive Switching Memory Devices *Scientific Reports*
- [43] Nishi Y 2014 *Advances in nonvolatile memory and storage technology* (Woodhead Publishing)